Microfluidic Array with Integrated Oxygenation Control for Real-Time Live-Cell Imaging: Effect of Hypoxia on Physiology of Microencapsulated Pancreatic Islets

Mohammad Nourmohammadzadeh[1,2*], Joe F Lo[3*], Matt Bochenek[1,2], Joshua E. Mendoza-Elias[1,2], Qian Wang[1,2], Ze Li[1,2], Liyi Zeng[1], Meirigeng Qi [1], David Eddington[2], José Oberholzer [1,2], Yong Wang[1,2]

[1] Department of Surgery/Transplant, University of Illinois at Chicago, Chicago, IL. 60612
[2] Department of Bioengineering, University of Illinois at Chicago, Chicago, IL. 60607
[3] Department of Mechanical Engineering, University of Michigan at Dearborn, Dearborn, Michigan. 48128

[*] Equal contribution

Supplementary Information

This document presents additional information concerning the design of the microfluidic device described in the manuscript as well as additional information about device fabrication, islet isolation, and fluorescence imaging.

Supplementary Table 1	**Geometry of the microfluidic array for microencapsulated pancreatic islets**
Supplementary Table 2	**Stimulation and oxygenation protocols**
Supplementary Figure 1	**Characterization of device oxygenation in the microfluidic islet trapping array** (**A**) 21-5-21% cyclic oxygenation diffusion property (n = 3, means ± SD). (**B**) 21-10-5-1% step-down oxygenation diffusion property (n = 3, means ± SD). (**C**) 21-5-21% cyclic oxygenation dissolving property (n = 3, means ± SD). (**D**) 21-10-5-1% step-down oxygenation dissolving property (n = 3, mean ± SD).

Calculation of pressure drop for designing microchannel geometry

In order to optimize the trapping efficacy for microcapsules, flow resistance of the straight and looped channels were calculated using the Dary-Weisbach equation, which was modified by Poiseuille's Law for a rectangular channel. The value of the Darcy friction factor *f* is related to the aspect ratio of the channel and Reynolds number, in a product expressed as $C(\alpha)=f^*Re$. After simplification, the following expression was used for resistance:

$$\Delta P = \frac{C(\alpha)}{32} * \frac{\mu L Q P^2}{A^3}$$ **Equation 1,**

were *α* is the aspect ratio, *L* is the length of the channel, *A* is the cross sectional area, *Q* is the flow rate, and *P* is the channel perimeter.

With no particles trapped, the straight channel and the loop channel share the same pressure input. If the resistance for the straight channel is less than that of the loop channel, then the volumetric flow will be greater, allowing a particle to be directed into the U-cup pocket.

$$\frac{Q_1}{Q_2} = \frac{C_2(\alpha_2)}{C_1(\alpha_1)} * \frac{L_2}{L_1} * \left(\frac{P_2}{P_1}\right)^2 * \left(\frac{A_1}{A_2}\right)^2 = \frac{C_2(\alpha_2)}{C_1(\alpha_1)} * \frac{L_2}{L_1} * \left(\frac{W_2 + H}{W_1 + H}\right)^2 * \left(\frac{W_1}{W_2}\right)^2 > 1$$ **Equation 2,**

Where $A = W * H$ and $P = 2(W + H)$; *H* is the height of the channels and W the width.

L_2 / L_1 and W_2 / W_1 are two important design parameters that determine the capture efficiency when the channel height is constant. For higher capture efficiency, it is desirable to maximize L_2 / L_1 and minimize W_2 / W_1; however, there are constraints in determining these dimensions. The width of path 1 (W_1) should be smaller than the diameter of the capsules in order to be an effective trap. On the other hand, the width of path 2 (W_2) and the channel height (*H*) should be larger than the capsule diameter to allow for continuous flow without clogging. However, *H* should also be short enough to minimize leakage around the immobilized particle, and prevent multiple particles trapping in a single trap. Based on our application, *H* should be set to $H \leq 1.5D$, where *D* is the diameter of the microcapsule. Our geometry is designed to be efficient at trapping capsules with diameters of 400 μm to 550 μm. Based on the calculation, the device geometry was derived as shown in supplementary table 1 to trap encapsulated islets.

Supplementary Table 1. Geometry of the microfluidic array for microencapsulated pancreatic islets

	Width (μm)	Height (μm)	Length (μm)
Top Layer: Perfusion Channel Path 1	175	600	75
Top Layer: Perfusion Channel Path 2	575	600	5000
Middle Layer: Gas Membrane		100	
Bottom Layer: Gas Channel		300	

Encapsulation in Ca^{2+}/Ba^{2+} Alginate Microbeads

Briefly, 1 mL of 2.0% (w/v) alginate (NovaMatrix, Sandvika, Norway: 63–67% G, MW 200 – 240 kDa) in 0.3 M mannitol (pH 7.2-7.4) was loaded into a 5 mL syringe. Isolated islets were then added to the syringe constituting a final suspension of 1.8% (w/v) alginate and islet solution. This suspension was dripped using a syringe pump and an electrostatic microbead generator (7 kV, flow: 10 ml/hr per 0.35 mm needle) over a period of 5 min, resulting in alginate microbeads of 400 – 550 μm in diameter in a gelling solution (50 mM $CaCl_2$ and 1 mM $BaCl_2$, pH 7.2-7.4). The microbeads were stirred in the gelling bath for another 5 min to ensure that the gel was saturated. The alginate microbeads were then washed and cultured in RPMI containing 10% FBS and 1% penicillin/streptomycin (Invitrogen, NJ) for 24 hrs culture at 37ºC and 5% CO_2.

Device fabrication

The 100 μm-thick gas-permeable PDMS membrane was made by spinning premixed 10:1 mass ratio of PDMS prepolymer to curing agent (Sylgard 184 kit, Dow Corning) on a thoroughly cleaned silicon wafer that is vacuum-adhered to a precision spinner (Laurel Technology, PA). The PDMS-coated wafer was spun at 900 RPM for 30 s. The PDMS-coated

wafer was then placed on a leveled hot plate set to 80ºC and heated for 2 hrs to cure the PDMS. The liquid and gas channel network were designed in AutoCAD and printed on high-resolution (16,000 dpi) transparency film (Fineline Imaging, CO). The transparency was used as a photomask to selectively crosslink photoresist prespun to a desired thickness on a silicon wafer. Briefly, SU-8 2150 photoresist (Microchem, MA) was spun to achieve a thickness of 600 μm and 300 μm for liquid channel and gas channel respectively, in accordance to the manufacturer's protocol. Following placement of the photomask, the photoresist was then exposed to UV light to polymerize and transfer the pattern to the SU-8. Finally, uncross-linked regions of photoresist were removed by washing the wafer in SU-8 developer solution. Once the SU-8 negative mold master was fabricated, PDMS was poured onto the master to generate a positive mold at the desired thickness. The PDMS mixture was cured for 2 hrs at 80ºC. After fabrication of the three components was completed, the device was assembled. The components were first cleaned with scotch tape. Then, the liquid channel layer and the gas permeable component were bonded after surface exposure to oxygen plasma and annealed on a hotplate at 80ºC for 1 hr while pressed with a 1 kg weight. Next, a cork-borer (gauge 11) was used to puncture inlet and outlet holes for the liquid and gas channels. Finally, the gas channel layer exposed to oxygen plasma was bonded to the other side of the gas permeable PDMS and annealed on a hotplate at 80ºC for 1 hr while pressed with a 1 kg weight.

Rat and human islet isolation

In brief, 15mL Collagenase type XI at a concentration of 2.2 mg/mL (Sigma, MO) was injected via the common bile duct into the pancreas and digested in a 37ºC water bath for 15 min. The digested tissue was then purified by discontinuous Ficoll density gradients (Mediatech Inc. Herndon, VA) through centrifugation for 15 min at 640 *g.* The purified islets

were cultured in RPMI containing 10% fetal calf serum (FBS), and 1% penicillin/streptomycin (Invitrogen, NJ) with glutamine, for 24 hrs at 37ºC. All experiments performed with animals were performed in accordance with protocols approved by the University of Illinois at Chicago Office of Animal Care and Institutional Biosafety Committee.

Human islets were isolated according to published literature In brief, cadaver pancreata were obtained from organ procurement organizations (OPO) with research consent. The pancreata were trimmed and distended with Collagenase and digested in a modified Ricordi chamber. After collection and wash steps, the digested tissue was further purified by a continuous UIC-UB gradient protocol [27] on a cell separator (Cobe 2991, Cobe Inc., Lakewood, CO) and then cultured in CMRL 1066 media at 5% CO_2 and 37ºC.

Fluorescence imaging

In brief, islets were incubated with 5 μM Fura-2 and 2.5 μM Rh123 for 30 min at 37ºC in KRB2. The islets were then washed with KRB2 for 10 min and loaded into the temperature equilibrated microfluidic device mounted on an inverted epifluorescence microscope (Leica DMI 4000B). KRB containing high glucose (14 or 25 mM) or KCl (30 mM) was then administered to the islets using gravity feed. Dual-wavelength Fura-2/AM was excited at 340 and 380 nm and fluorescent emission was detected at 510 nm. Intracellular Ca^{2+} was expressed as a ratio of fluorescent emission intensity F340 /F380 (%). Rh123 was excited at 490 ± 10 nm, and emission was measured at 530 ± 10 nm. Fura-2 and Rh123 fluorescence emission spectra were filtered using a Fura-2/FITC polychroic beamsplitter and double band emission filter (Chroma Technology. Part number: 73100bs). These images were collected with a CCD (Retiga-SRV, Fast 1394, QImaging). SimplePCI software (Hamamatsu Corp.) was used for image acquisition and analysis. Both fluorescence signals were expressed as

'change-in-percentage' after being normalized against basal intensity levels established before stimulation. The reduced forms of NAD and NADP, designated NAD(P)H, were measured using the same imaging system. The autofluorescence of NAD(P)H was excited at 365 nm and measured at 495 nm in dye-free islets.

Stimulation and oxygenation protocols used in hypoxia studies were listed as follow

Supplementary Table 2. Stimulation and oxygenation protocols as shown

Step Number	Condition	[Glucose] (mM)	O_2 (%)	Time (min)
1.	Control-LOW	2	21	10
2.	Control-High	14/rat, 25/human	21	15
3.	Return to baseline	2	21	15
4.	Hypoxia 1 pre-culturing	2	10	15
5.	Hypoxia 1 stimulus	14/rat, 25/human	10	15
6.	Return to baseline	2	21	15
7.	Hypoxia 2 pre-culturing	2	5	15
8.	Hypoxia 2 stimulus	14/rat, 25/human	5	15
9.	Return to baseline	2	21	15
10.	Hypoxia 3 pre-culturing	2	1	15
11.	Hypoxia 3 stimulus	14/rat, 25/human	1	15
12.	Return to baseline	2	21	15

Device oxygenation capability

In diffusive mode, as shown in Supplementary Figure 1A and 1B, the device was capable of creating and maintaining the targeted oxygen concentrations with high consistency. In cyclic oxygenation protocol (21-5-21%), the time needed to switch from 21% to 5% oxygen concentration was less than 40 s as was the reversion back to 21% from 5%. Equally important, both concentrations were able to be well-maintained overtime (21.21% ± 0.05 and 6.22% ± 0.03). Similarly, the time needed to change from one oxygen concentration to another

in step-down protocol was also less than 40 s and again was well-maintained overtime (21.33% ± 0.04, 11.53% ± 0.05, 6.33% ± 0.02, and 1.77% ± 0.02, respectively).

In dissolved mode shown in Supplementary Figure 1C and 1D, the time needed to switch from 21% (22.07% ± 0.13) to 5% (6.83% ± 0.08) was approximately 120 s, that was longer than in the diffusion mode, similar to the observation made in our previous published device [21]. Similarly, the time needed to change from a particular oxygen concentration to another in the step-down protocol was less than 120 s and was stably maintained (20.87% ± 0.06, 11.63% ± 0.03, 6.45% ± 0.03, and 1.68% ± 0.03, respectively). It is worth noting that the oxygen sensor used in the oxygen evaluation has a measuring delay-time (τ) of 15-20 s in gas and 30-45 s in aqueous media. In reality, the oxygenation time is probably much faster than what was observed. Additionally, the exact concentrations of the oxygen tanks used in this study did not precisely correlate with the manufacturers labels and there was a 0.3-1.0% variation in the concentration.

Supplementary Figure 1 . Characterization of device oxygenation in the microfluidic islet trapping array

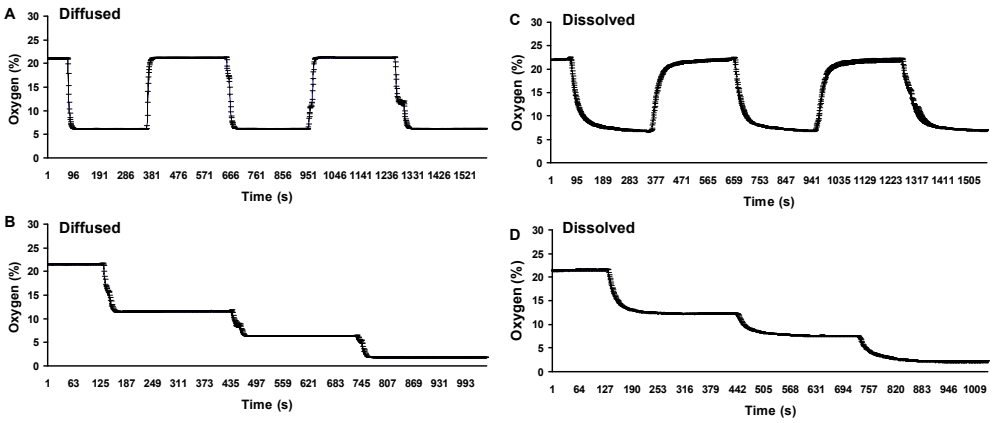

Loading and trapping efficacy of microcapsulated islets

Comparable to previously reported hydrodynamic traps, the device design allows for a high trapping efficacy for microencapsulated islets with a specific size of 400-550 μm in diameter. Additionally, the device fabrication is straightforward in comparison to well-established methods. It has to be noted that the insertion of a serpentine channel, before the trapping area, greatly facilities the loading mechanism and increases the trapping efficacy as well as the hydrostatic-driven feed without the need of syringe pumps. Shear stress is considered a major concern when designing a hydrodynamic trap, since the fluidic restrictions at the trap interface are the site of highest shear stress during cell loading and during perfusion. Since shear stress scales linearly with the velocity, the hydrostatic-driven feed used for the capsule loading greatly reduces this shear stress as indicated with the normal morphology of the microcapsule.